EUROPEAN ORGANIZATION FOR NUCLEAR RESEARCH

CERN – SL DIVISION

SL-Note-2000-09 OP

Orbit Steering and Central Frequency for LEP2 Energy Calibration

J. Wenninger

Abstract

The central frequency is an important parameter of the LEP beam energy model. It is a direct measurement of the LEP circumference and is used to evaluate the contribution of the quadrupoles to field integral relevant for the LEP beam ebergy. Its evolution over a run is tracked using direct frequency measurements combined with radial beam position measurements in the LEP arcs. The influence of orbit corrections on the central frequency measurement techniques was evaluated and a model allowing to correct for changes of corrector settings was developped. The central frequency data for the LEP2 runs between 1996 and 1999 was re-analysed to include corrections due to the closed orbit steering.

Geneva, Switzerland

February 2, 2000

1 Introduction

The LEP beam energy is measured with an accuracy of 0.5 MeV using resonant depolarization (RDP) for beam energies up to 61 GeV [1, 2, 3]. So far the level of transverse polarization observed at higher energies was not sufficient to perform resonant depolarization. For LEP2 the RDP calibrations are interpolated to beam energies above 80 GeV using NMR probes [3], the LEP flux-loop [3], the LEP spectrometer [4] or the relation between the synchrotron tune and the RF voltage [5]. Both the interpolation and the tracking of the beam energy during a LEP run require a proper modelling of the various sources of energy changes. Terrestrial tides [6, 7] and slow geological deformations [7] modify the LEP circumference and affect the LEP beam energy in a significant way. The length of the central orbit, which is equivalent to the LEP circumference, is an important ingredient of the energy model and must be tracked for each fill of a LEP run.

This note describes the measurement of the central orbit length (or central RF frequency) at LEP. Systematic effects due to the orbit steering will be addressed and a model for the influence of steering will be presented. Finally the central frequency data for the LEP runs from 1996 to 1999 will be reviewed.

2 Beam Energy and Central Frequency

In a storage ring the beam energy is defined by the integral on the bending magnetic field B

$$E = \frac{ec}{2\pi} \oint B\, ds = 47.7[\mathrm{MeV/Tm}] \oint B\, ds \tag{1}$$

with e the electron charge and c the speed of light. For a beam travelling on an orbit with a length C the beam energy can be expressed as

$$E = E_d + E_q + E_\epsilon \tag{2}$$

where E_d and E_q are respectively the contributions of the dipoles and the quadrupoles to the beam energy. They are given by

$$E_d = \frac{ec}{2\pi}(BL)_d \quad \text{and} \quad E_q = -\frac{1}{\alpha}\frac{C - C_c}{C} \tag{3}$$

E_d depends on the integrated dipole field $(BL)_d$ and accounts usually for more than 99.8% of the beam energy. E_q is a function of the momentum compaction factor α, of the actual orbit length C and of the length of the central orbit C_c (the LEP machine circumference). In general E_q does account for more than $\pm\,0.2\%$ of the field integral. On the central orbit the beam is centred on average in the quadrupoles and E_q vanishes. Other elements (for example horizontal correctors) can give additional small contributions E_ϵ to the energy.

At LEP the particles are ultra-relativistic and the length C of their orbit is determined by the frequency of the RF system f_{RF} which are related through

$$f_{RF} = h\frac{c}{C} \tag{4}$$

with h the RF harmonic number. The RF frequency corresponding to the central orbit is called the central frequency f^c_{RF}. At LEP the operating RF frequency f_{RF} of 352.25 MHz never differs from f^c_{RF} by more than $\pm\,200$ Hz. For this reason only the last 4 digits of the (central) RF frequency will be quoted throughout this document.

At LEP the absolute beam energy calibration is always obtained from resonant depolarization. To track the beam energy on a fill by fill basis, NMR probes are cross-calibrated with RDP between 40 and

61 GeV [3]. Ideally the probes should sample the dipole field in an unbiased way and be able to track E_d. Since NMR probes are not sensitive to E_q (and E_e), the evolution of C_c must be known to compare NMRs and RDP data over long time intervals and to model the beam energy for every fill. C_c is usually tracked using the beam position measurement in the LEP arcs [7, 2, 3]. The average radial beam position at up to 240 arc monitors, denoted by X_{arc}, is related to the circumference and RF frequency through the horizontal dispersion D_A at the monitors :

$$\Delta X_{arc} = -\frac{D_A}{\alpha}\frac{\Delta C_c}{C_c} \simeq 0.11\ \Delta C_c \tag{5}$$

$$\Delta X_{arc} = \frac{D_A}{\alpha}\frac{\Delta f^c_{RF}}{f^c_{RF}} \simeq 8.4[\mu\mathrm{m/Hz}]\ \Delta f^c_{RF} \tag{6}$$

The numerical coefficients may vary by a few percent for different optics. Direct measurements of the central frequency are used to obtain an absolute calibration of X_{arc}. It is not necessary to know the absolute value of C_c (resp. f^c_{RF}) with high accuracy since a constant measurement offset can be absorbed in the definition of E_d without significant bias to the beam energy model.

For a perfectly aligned machine the definition of the central frequency (and of the central orbit length) is unambiguous. It corresponds to the RF frequency (or orbit length) for which the beam is centred in all quadrupoles. In a real machine with misaligned magnets the beam is travelling on a closed orbit that is in general never centred in each quadrupole. In such a case the central frequency corresponds to the RF frequency for which the beam is centred on average in the quadrupoles. Since the central frequency must be measured with the beam, the actual measurement result may depend on the beam steering through the quadrupoles. The study of the sensitivity of the central frequency on details of the closed orbit is the main subject of this note.

3 Direct Central Frequency Measurements

Two experimental techniques are used to determine the central frequency at LEP. Both methods use the fact that the tune is independent of the sextupole strength (or chromaticity) when the beam is centred in the sextupoles. At LEP each sextupole-quadrupole pair is mounted on one girder and the magnetic axis of the two magnets are aligned with a tolerance of 0.2 mm RMS. Centring the beam in the sextupoles or the quadrupoles is therefore (almost) identical. In LEP there are 240 SF sextupoles installed next to horizontally focusing quadrupoles and 256 SD sextupoles installed next to vertically focusing quadrupoles.

The relative alignment between sextupoles and quadrupoles sets an intrinsic limit to the absolute accuracy of the central frequency. The error on the central frequency σ_f is related to the alignment RMS σ_{SQ} by

$$\sigma_f \simeq f_{RF}\frac{\sigma_{SQ}}{\bar{\rho}\sqrt{N_S}} \simeq 4.6[\mathrm{Hz/mm}]\ \sigma_{SQ} \tag{7}$$

where $\bar{\rho}$ is the average bending radius, f_{RF} is the typical (central) RF frequency and N_S is the number of sextupoles. The alignment accuracy of $\sigma_{SQ} \simeq 0.2$ mm leads to an uncertainty on the central frequency of approximatively $\pm$ 1 Hz.

3.1 Measurement Techniques

A first measurement technique uses the principle of *RF frequency shaking* [8]. The RF frequency is repeatedly swept according to a predefined function over a range of 50 to 100 Hz. If the chromaticity is non-zero the horizontal tune Q_h is modulated by the RF frequency function as shown in Figure 1. Q_h is

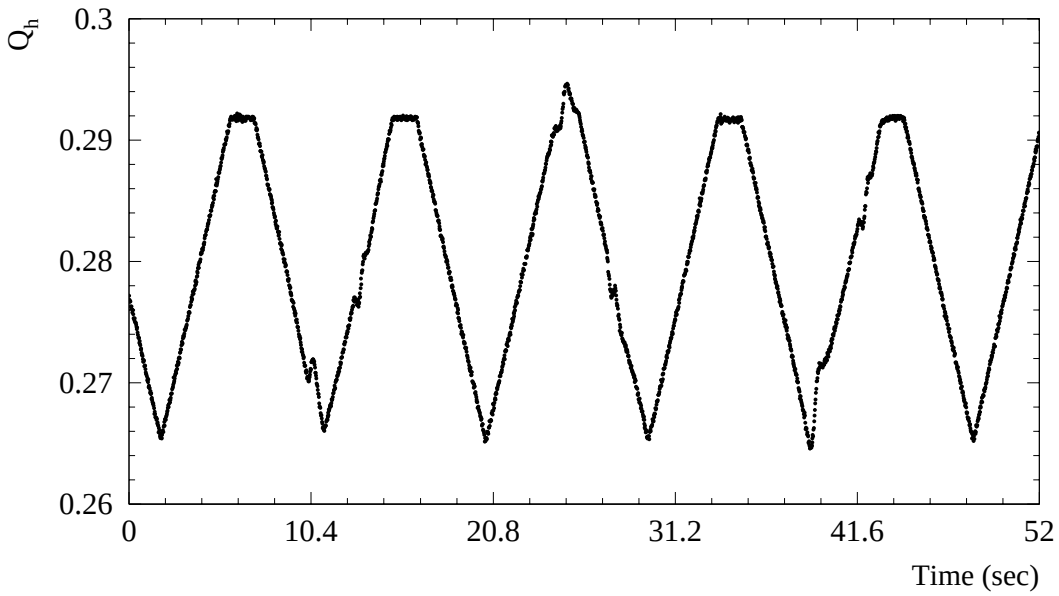

Figure 1: Time dependence of the horizontal tune Q_h during a central frequency measurement by RF frequency shaking. Q_h follows the modulation of the RF frequency which is repeatedly cycled between two values, with a short plateau at the lower frequency. The amplitude of the tune change is directly proportional to the chromaticity and to the frequency sweep. The periodic tune perturbations (spikes) are due to the 14.4 second SPS cycle.

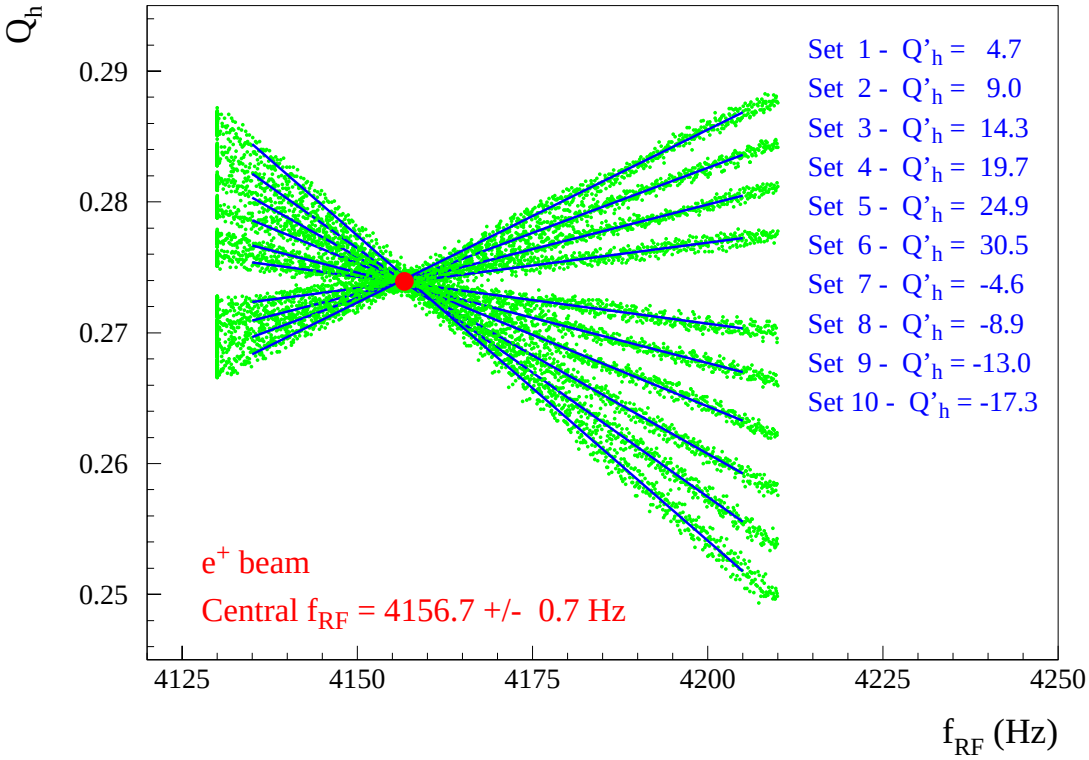

Figure 2: Central frequency measurement using the method of RF frequency shaking. The tune dependence on RF frequency is reconstructed for each measurement, the slope being proportional to the chromaticity Q'_h (see example of Figure 1). At the crossing point of all measurements the beam is centred in the sextupoles since the tune is independent of Q'_h : this frequency setting corresponds to the central frequency (only the last 4 digits are given).

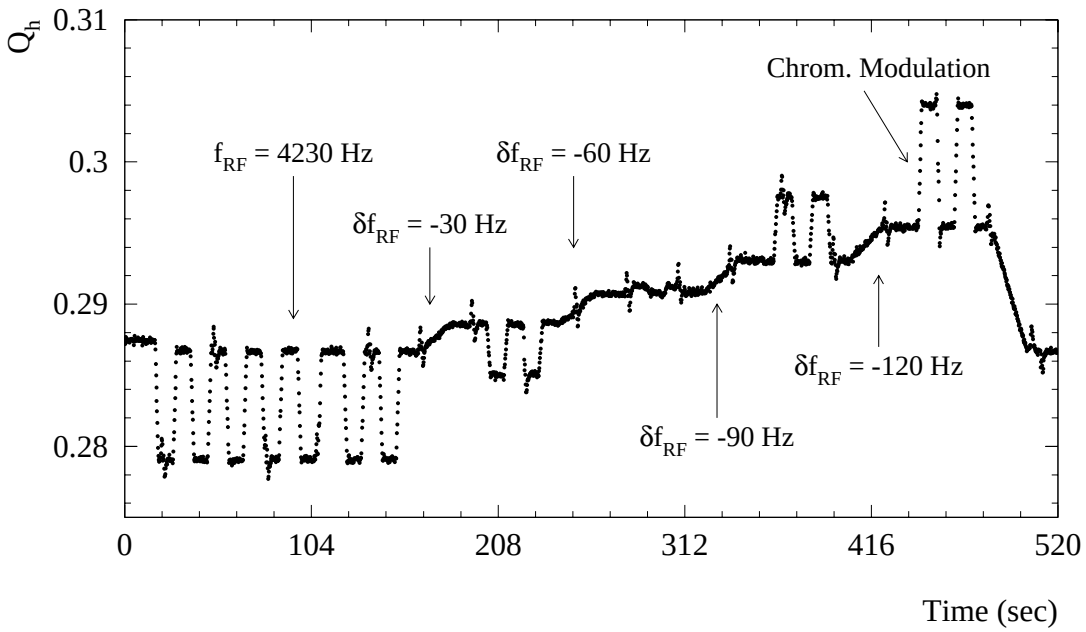

Figure 3: Evolution of the horizontal tune Q_h during a central frequency measurement by sextupole modulation. The step-wise changes of Q_h correspond to a chromaticity modulation of 8 units which is repeated twice for each RF frequency setting. At the start of the measurement the sextupoles are modulated 5 times to obtain a stable cycle. The RF frequency steps are indicated by arrows. The tune change almost vanishes for a frequency trim of -60 Hz. The periodic perturbations of Q_h are due to the 14.4 second SPS cycle.

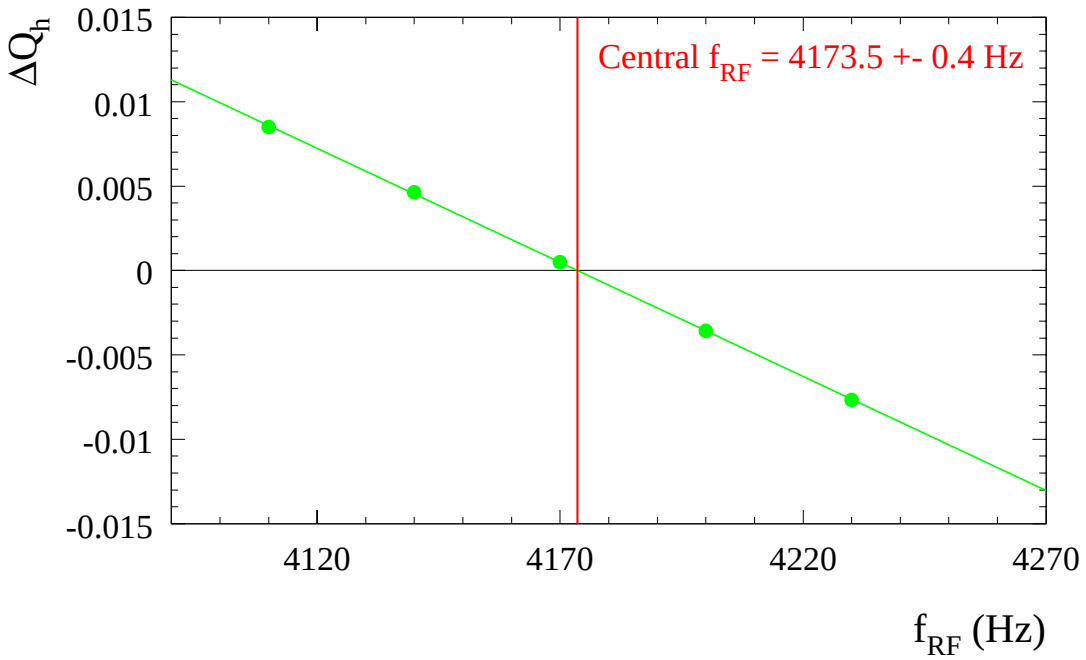

Figure 4: Horizontal tune change ΔQ_h due to the chromaticity modulation as a function of the RF frequency. The data corresponds to the measurement shown in Figure 3. The error on ΔQ_h is smaller than the symbol size. The central frequency corresponds to $\Delta Q_h = 0$.

continuously tracked in a PLL (Phase Locked Loop) mode and its dependence on RF frequency can be reconstructed from the known frequency function using a cross-correlation analysis. The measurement is repeated for different chromaticity settings to find the frequency setting for which Q_h is independent of the chromaticity as indicated in Figure 2.

A second measurement technique is based on the principle of *sextupole modulation* where the chromaticity is varied between two settings typically separated by about 5 to 10 units. The tune change corresponding to this chromaticity difference is measured for a few settings of the RF frequency as shown in Figure 3. A straight line fit to the tune change versus RF frequency yields the central frequency (Figure 4).

The accuracy of the two methods varies between 0.2 and 2 Hz and depends on beam conditions and machine stability. The measurement technique based on RF frequency shaking is more delicate and requires a very stable tune over a time interval of at least 15 minutes. Slow tune drifts bias the crossing point of the curves shown in Figure 2. For this reason the second method, which is faster and more robust, has been preferred for LEP2.

4 Central Frequency and Closed Orbit Distortions

When the ideal orbit is distorted by a single dipole kick θ, the closed orbit distortion u is a function of the path length s along the ideal orbit given by :

$$u(s) = \frac{\sqrt{\beta_u(s_0)\beta_u(s)}}{2\sin(\pi Q)} \cos(|\phi_u(s) - \phi_u(s_0)| - \pi Q)\, \theta \tag{8}$$

$\beta_u(s)$ and $\phi_u(s)$ are the betatron function and the betatron phase. Q is the machine tune. s_0 is the longitudinal position of the kick θ. This expression is valid in both transverse planes ($u = x, y$). A single horizontal kick θ does not add to the bending of the dipole magnets since the kick is compensated by the lattice on the closed orbit. This statement can be generalised for a set of correctors as long as the kicks are incoherent and do not all add up systematically in the same direction, in which case they would contribute directly to the dipole field.

In a section where the curvature ρ is locally constant, the beam position can be expressed in polar coordinates $r = \rho + u$ and ϕ. While the path length on the ideal orbit is $ds = \rho d\phi$, the path length dl on the distorted orbit becomes (Figure 5) :

$$dl = \sqrt{r^2 + \left(\frac{dr}{d\phi}\right)^2}\, d\phi \tag{9}$$

The change of path length dL due to the distortion

$$dL = dl - ds = \sqrt{r^2 + \left(\frac{dr}{d\phi}\right)^2}\, d\phi - ds \tag{10}$$

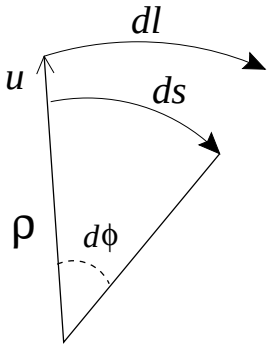

Figure 5: Path lengths on the ideal (ds) and on the distorted (dl) orbit.

can be expanded to yield

$$dL \approx \left(\frac{u}{\rho} + \frac{1}{2} \left(\frac{du}{ds} \right)^2 \right) ds \tag{11}$$

where only the leading terms have been kept. The total path length change Λ due to the closed orbit distortion is obtained by integration over the ring,

$$\Lambda = \oint dL = \Lambda_1 + \Lambda_2 \tag{12}$$

where Λ has been split into a linear lengthening Λ_1 and a quadratic lengthening Λ_2 [9] :

$$\Lambda_1 = \oint \frac{u}{\rho} \, ds \qquad\qquad \Lambda_2 = \frac{1}{2} \oint \left(\frac{du}{ds} \right)^2 \, ds \tag{13}$$

Λ_1 is related to the orbit position shift and Λ_2 to the orbit RMS, and in general $\Lambda_2 << \Lambda_1$. When Λ_1 is evaluated for the closed orbit distortion given by Equation 8, it reduces to a simple expression which depends only on the local dispersion D_u and the kick θ [9, 10] :

$$\Lambda_1 = D_u(s_0) \, \theta \tag{14}$$

Only horizontal correctors in the arcs and in the dispersion suppressors contribute to Λ_1 since the dispersion vanishes in the straight sections and in the vertical plane. For a combination of N_C kicks θ_j at locations with horizontal dispersion D_{xj} we obtain :

$$\Lambda_1 = \sum_i^{N_C} D_{xj} \theta_j \tag{15}$$

because the orbit displacements add up linearly as long as they are not excessively large.

Earlier simulations of the effect of correctors on the beam energy have shown that the small contributions due to Λ_2 are cancelled by the sextupoles [10]. The RF frequency constrains the length of the orbit to remain constant and the beam must change its average radial position to accommodate the lengthening Λ_1. This in turn leads to a change of the average beam energy E :

$$\frac{\delta E}{E} = -\frac{1}{\alpha} \frac{\Lambda_1}{C} = -\frac{1}{\alpha C} \sum_i^{N_C} D_{xj} \theta_j \tag{16}$$

As a consequence of such a radial movement one might naively expect that the *measured* central frequency should change by

$$\delta f^c = -\frac{\Lambda_1}{C} f^c_{RF} \tag{17}$$

since δf^c is exactly the frequency change that must be applied to compensate the radial movement due to Λ_1 and re-centre the beam in the quadrupoles. The shift δf^c would be a purely experimental bias due to the fact that f^c_{RF} must measured with the beam. Such an apparent change of the measured central frequency would imply that energy changes due to corrector settings and f^c_{RF} are strongly correlated and must be treated carefully in the energy model to avoid double counting of corrections. This argument does not take into account the detailed effect of the closed orbit change and the way the sextupole sample the orbit.

4.1 Model of the Influence of Orbit Steering on Central Frequency Measurements

To understand the relation between orbit kicks and central frequency *measurements* we must analyse the tune changes induced by the orbit distortions in the sextupoles. To first order the horizontal beam position change δx_i at the i^{th} sextupole receives contributions δx_i^{β} from the betatron oscillation and $\delta x_i^{\delta p}$ from the radial movement

$$\delta x_i = \delta x_i^{\beta} + \delta x_i^{\delta p} = \sum_j^{N_C} \frac{\sqrt{\beta_{xi}\beta_{xj}}}{2\sin(|\pi Q|)} \cos(|\Delta\phi_{ij}| - \pi Q)\ \theta_j + D_{xi}\frac{\delta E}{E} \tag{18}$$

where $\Delta\phi_{ij}$ is the betatron phase between i^{th} sextupole and j^{th} corrector. $\frac{\delta E}{E}$ is the relative energy change given in Equation 16. β_{xi} is the horizontal betatron function and D_{xi} is the horizontal dispersion at the i^{th} sextupole. The horizontal tune change due to the position shifts in the N_S sextupoles is :

$$\delta Q_\theta = \frac{1}{4\pi}\sum_i^{N_S} K_{2i} l_i \beta_{xi} \delta x_i \tag{19}$$

K_{2i} is the strength and l_i the length of the i^{th} sextupoles. Substituting the expressions for δx_i and $\delta E/E$ the tune change can be written

$$\delta Q_\theta = -Q'_S \sum_j^{N_C} \frac{D_{xj}\theta_j}{\alpha C} + \sum_j^{N_C} \sqrt{\beta_{xj}} P_{Sj}\theta_j \tag{20}$$

with Q'_S the contribution of the sextupoles to the horizontal chromaticity

$$Q'_S = \frac{1}{4\pi}\sum_i^{N_S} K_{2i} l_i \beta_{xi} D_{xi} \tag{21}$$

and

$$P_{Sj} = \frac{1}{8\pi\sin(|\pi Q|)} \sum_i^{N_S} K_{2i} l_i \beta_{xi}^{3/2} \cos(|\Delta\phi_{ij}| - \pi Q) \tag{22}$$

Horizontal and vertical chromaticity trims (increments) are given by

$$\Delta Q'_h = \frac{1}{4\pi}\left(\Delta K_2^{SF}\sum_i^{N_{SF}} l_i\beta_{xi}D_{xi} + \Delta K_2^{SD}\sum_i^{N_{SD}} l_i\beta_{xi}D_{xi}\right) \tag{23}$$

$$\Delta Q'_v = -\frac{1}{4\pi}\left(\Delta K_2^{SF}\sum_i^{N_{SF}} l_i\beta_{yi}D_{xi} + \Delta K_2^{SD}\sum_i^{N_{SD}} l_i\beta_{yi}D_{xi}\right) \tag{24}$$

with $\Delta K_2^{SF(D)}$ the strength changes of the $N_{SF(D)}$ sextupoles belonging to the SF(D) family. For a purely horizontal chromaticity change ($\Delta Q'_v = 0$) the strengths of the SD and SF families must satisfy :

$$r = \frac{\Delta K_2^{SD}}{\Delta K_2^{SF}} = -\frac{\sum_i^{N_{SF}} l_i\beta_{yi}D_{xi}}{\sum_i^{N_{SD}} l_i\beta_{yi}D_{xi}} \tag{25}$$

Following the orbit change due to the steering, the shift δf^c of the *measured* central frequency is determined by the condition that the total tune change due to the frequency change and kicks

$$\Delta Q_{tot} = -\frac{\delta f^c}{\alpha f_{RF}} Q'_S + \delta Q_\theta \tag{26}$$

should be independent of the chromaticity setting. For a horizontal chromaticity change ($dQ'_S = dQ'_h$) this conditions can be expressed as :

$$\frac{d(\Delta Q_{tot})}{dQ'_S} = 0 = -\frac{\delta f^c}{\alpha f_{RF}} - \sum_j^{N_C} \frac{D_{xj}\theta_j}{\alpha C} + \sum_j^{N_C} \sqrt{\beta_{xj}} \frac{dP_{Sj}}{dQ'_S}\theta_j \tag{27}$$

Using Equations 23 and 25 and solving for δf^c we obtain :

$$\delta f^c = \sum_j^{N_C} \theta_j F_j = \sum_j^{N_C} \theta_j (F_j^\delta + F_j^\beta) \tag{28}$$

where

$$F_{\delta j} = -f_{RF}\frac{D_{xj}}{C} \tag{29}$$

$$F_{\beta j} = \alpha f_{RF}\beta_{xj}\frac{B_j^{SF} + rB_j^{SD}}{A^{SF} + rA^{SD}} \tag{30}$$

$$A^{SF(D)} = \sum_i^{N_{SF(D)}} l_i \beta_{xi} D_{xi} \tag{31}$$

$$B_j^{SF(D)} = \frac{1}{2\pi \sin(|\pi Q|)} \sum_i^{N_{SF(D)}} l_i \beta_{xi}^{3/2} \cos(|\Delta\phi_{ij}| - \pi Q) \tag{32}$$

The expression in Equation 28 is a simple linear function of the kicks weighted by an optics dependent factor F. Equation 28 is only valid in the limit of small orbit variations (RMS change $\leq$ few mm). The term associated to F^δ corresponds to the effect of the orbit lengthening (see also Equation 17) :

$$\sum_j^{N_C} \theta_j F_j^\delta = -\frac{\Lambda_1}{C} f_{RF}^c \tag{33}$$

The sensitivity factors F^β, F^δ and F can be evaluated directly for any optics. They are shown for the $102^\circ/90^\circ$ and $60^\circ/60^\circ$ optics in Figures 6 and 7. The contribution F^β due to the betatron oscillations cancels on average the systematic contribution of F^δ which vanishes in areas where the dispersion is zero. When it is averaged over all correctors, F is very close to 0. The frequent sign changes of F prevent large shifts in f_{RF}^c when kicks from correctors or misaligned quadrupoles generate large lengthenings Λ_1 because they are oriented preferentially in one direction (inwards or outwards).

The shift of the closed orbit also influences the average beam position in the arcs that is used to track the central frequency for every fill. The shift of X_{ARC} is :

$$\delta X_{ARC} = \sum_j \theta_j G_j \tag{34}$$

where

$$G_j = -\frac{D_{xj}D_A}{\alpha C} + \frac{\sqrt{\beta_{xj}\beta_A}}{2N_M \sin(|\pi Q|)} \sum_i^{N_M} \cos(|\Delta\phi_{ij}| - \pi Q) \tag{35}$$

β_A is the horizontal betatron function and D_A the horizontal dispersion at the arc BPMs. N_M is the total number of monitors.

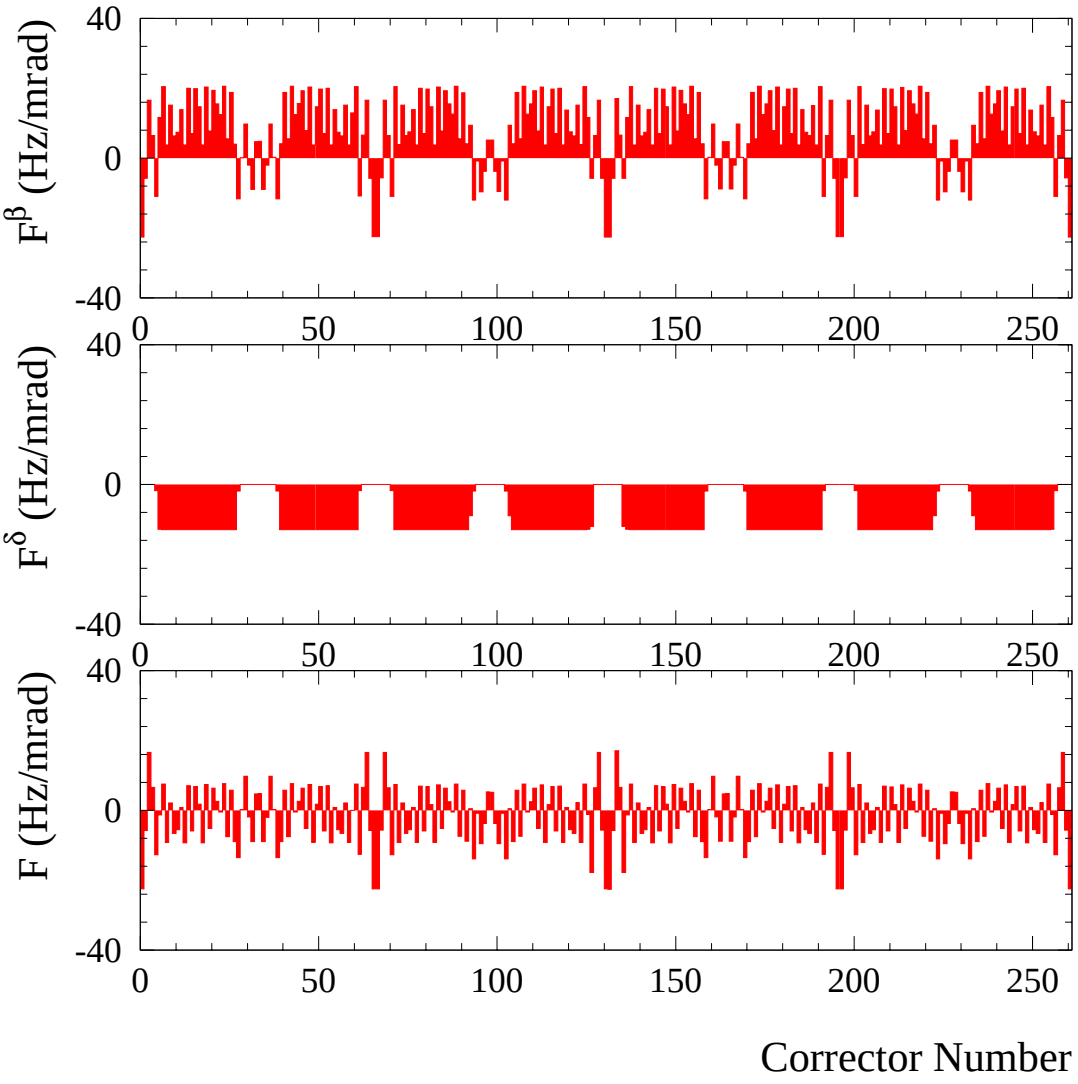

Figure 6: Sensitivity factors F^β, F^δ and F for all correctors with the $102°/90°$ optics (β_x^* = 1.5 m).

4.2 Model Tests with Simulations and Experiments

The validity of the analytical model was tested with simulations using the MAD program [11]. For a given optics and machine misalignment, the orbit is corrected using different corrector settings to RMS values ranging between 0.3 and 0.7 mm which are typical for LEP. For each correction the central frequency obtained by simulating the real measurement process is compared to the shift predicted by Equation 28. Figure 8 shows the results for two different LEP lattices. The predicted and measured central frequency shift are always well correlated. Obviously the absolute value of the central frequency cannot be predicted from the model since the quadrupole misalignment is unknown.

The central role of sextupoles in protecting the central frequency measurement against biases from corrector settings can be demonstrated by the simulation of a closed bump shown in Figure 9. A horizontal closed bump is arranged over two arc cells with a sextupole close to the maximum of the bump. The linear orbit lengthening Λ_1 generated by the correctors is large and scales with the bump amplitude. Due to the non-linearity of the sextupole, the bump must be precisely re-matched for each amplitude. When the sextupole is on at the nominal strength, the central frequency depends only weakly on the bump amplitude, but as soon as the sextupole is switched off, the central frequency shows a strong dependence on bump amplitude. This simulation shows that the central frequency is not very sensitive to

steering as long as the sextupoles sample the orbit sufficiently in areas where the dispersion is non-zero and where corrector kicks can produce a lengthening Λ_1.

In 1998 an experiment was carried out to test the validity of the model in LEP. The central frequency was first measured over a time interval of one hour and found to be stable within the measurement accuracy after correction for the tidal distortions. The orbit was then corrected towards a new target orbit for which a central frequency shift of -1 Hz was predicted from the model. A naive estimate based only on the orbit lengthening Λ_1 (Equations 17 and 33) would have yielded a change of -7.5 Hz. The measurement in in good agreement with the complete model.

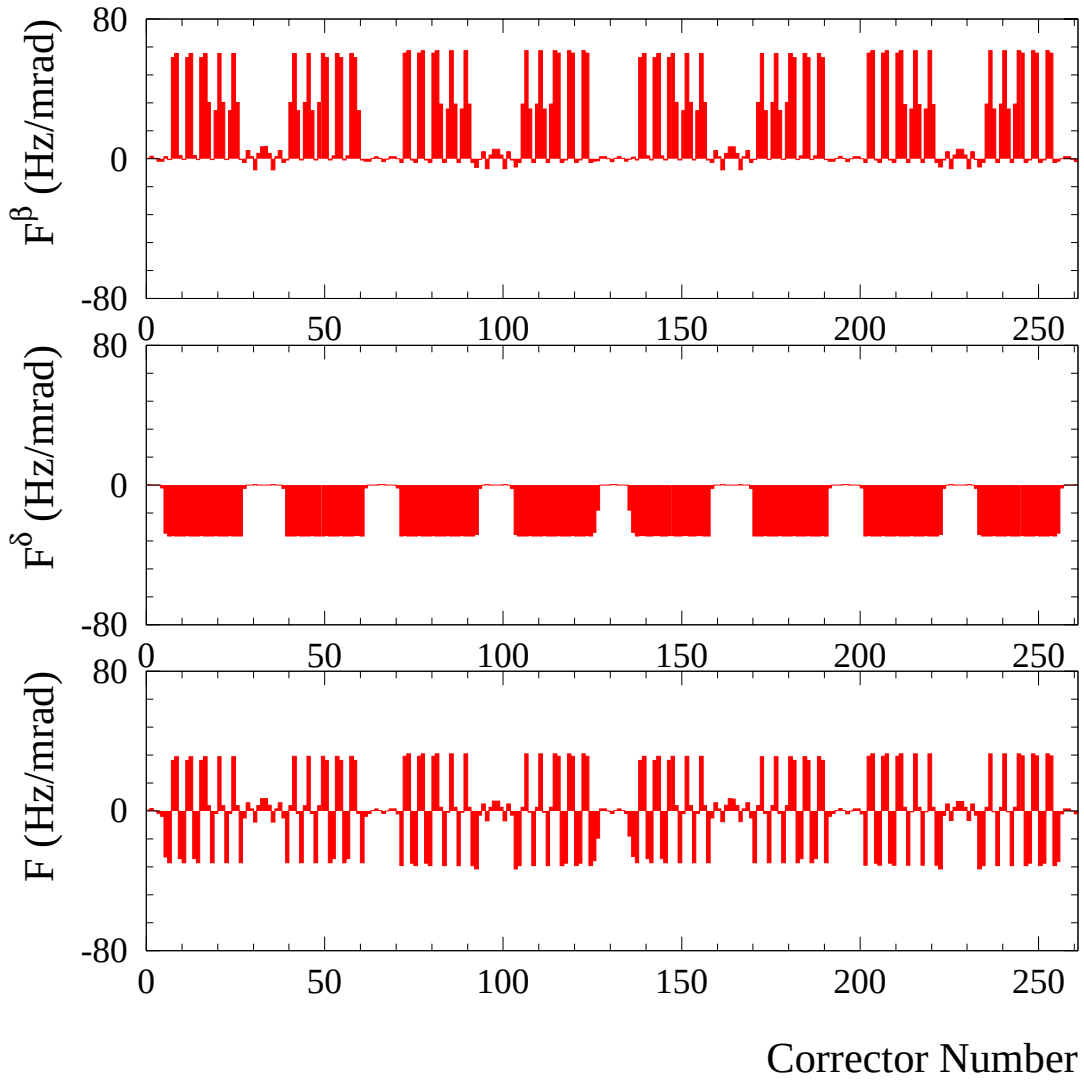

Figure 7: Sensitivity factors F^β, F^δ and F for all correctors with the $60°/60°$ optics.

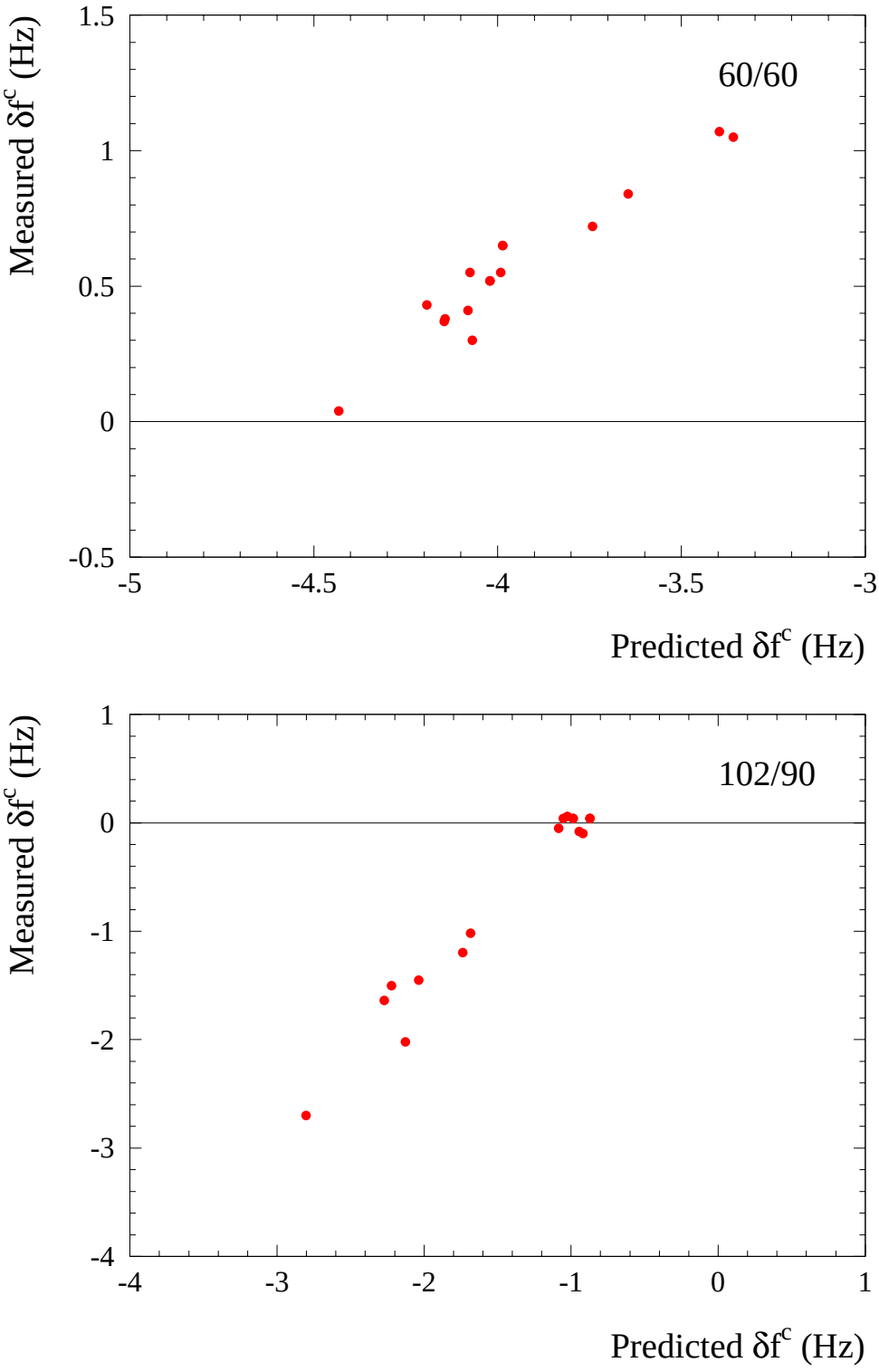

Figure 8: Simulation of the influence of corrector settings on the measured central frequency for a $60°/60°$ and a $102°/90°$ optics with a fixed horizontal quadrupole misalignment. The shift of the central frequency measurement (vertical axis) is shown as a function of the change predicted from Equation 28. Each points corresponds to a different corrector setting. The model predicts the relative changes with a good accuracy.

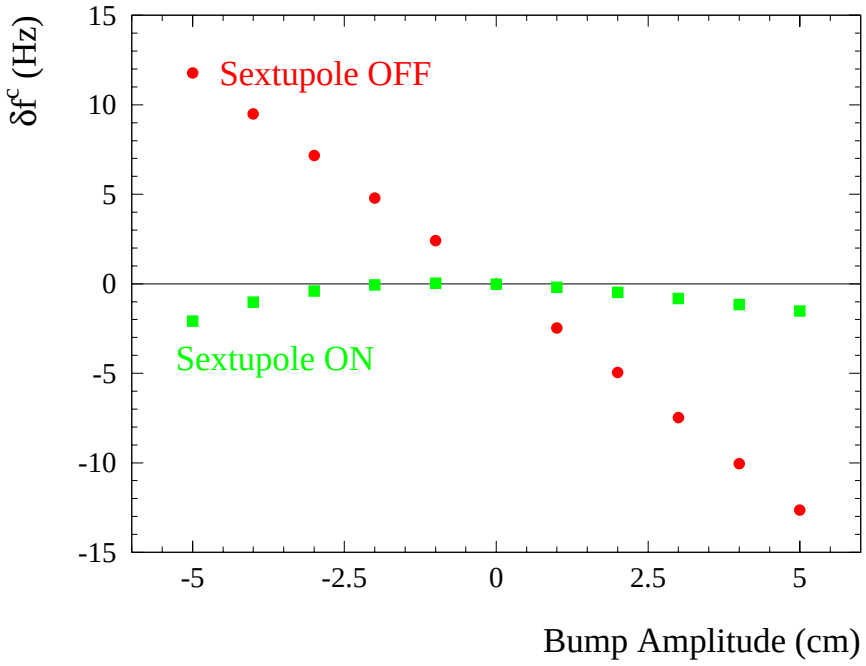

Figure 9: Simulation of the measured f^c_{RF} shift δf^c due to a closed local bump in the arcs for a $102°/90°$ optics. The local horizontal bump extends over two arc cells with an SF sextupole close to the bump maximum. The shift δf^c is given as a function of the bump amplitude when the sextupole in the bump is on or off. When the sextupole is off the orbit lengthening produces large f^c_{RF} shifts.

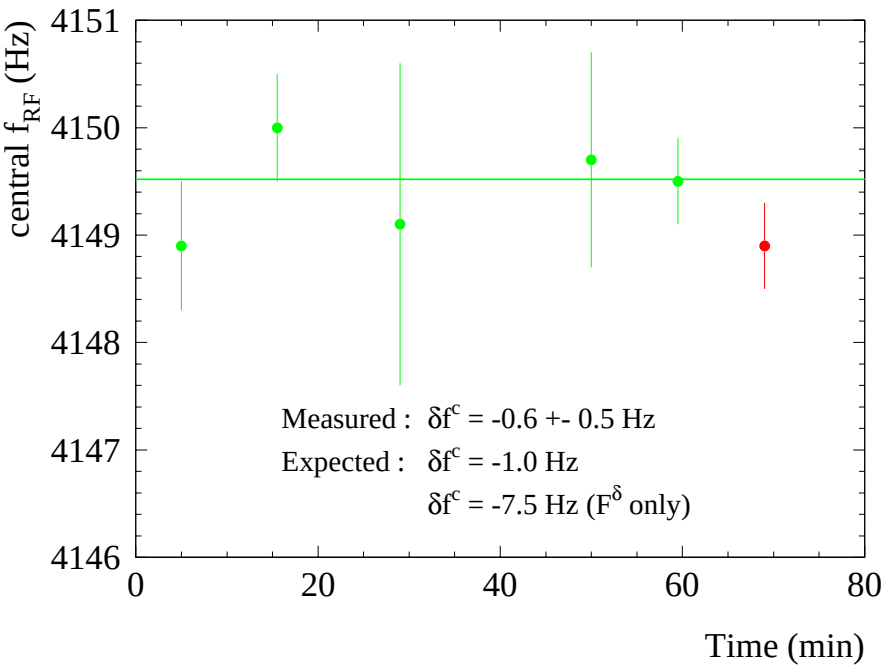

Figure 10: Experimental test of the influence of orbit steering on the f^c_{RF} measurement. For the last data point the orbit was corrected towards a different target and from the resulting corrector settings change a shift of -1 Hz was predicted from the model (Equation 28), in good agreement with the measurement. If only the orbit lengthening effect is taken into account (F^δ in Equation 28) the shift should be -7.5 Hz, in clear contradiction to the measurement.

5 Central Frequency at LEP2

The central frequency data for the LEP runs from 1996 to 1999 was reanalysed and corrected for the measurement shifts due to changes of corrector settings and closed orbits over the year. All data is corrected for the periodic effects of the terrestrial tides [6]. The evolution of the central frequency over one year is obtained primarily from the X_{arc} data which is available for almost every fill and normalised to the central frequency data. From the known corrector settings, the bias on X_{arc} (Equation 34) and on f^c_{RF} (Equation 28) can be easily evaluated. Only the relative change of the corrections over each run was applied. Long term drifts and absolute shifts of the corrections were not taken into account : to be meaningful an absolute correction would also require input from the quadrupole kicks due to alignment errors. The corrections lead to a reduced fill-to-fill scatter of the X_{arc} data, particularly for 1996 and 1997 where the reference orbits (and therefore also the corrector settings) for physics were changed frequently. The agreement between the evolutions of X_{arc} and f^c_{RF} is also improved.

The horizontal quadrupole movements over a run are unknown and delicate to unfold. Systematic drifts of f^c_{RF} measurements due to ground motion must be estimated by comparing X_{arc} and direct measurements over a run as they will be affected differently by the kicks from moving quadrupoles. Inspection of the data shows that direct measurements and X_{arc} agree within $\pm\,2$ Hz. Table 1 gives the momentum compaction factor and the sensitivity of the beam energy to central RF frequency at 100 GeV. Central frequency errors of $\pm\,2$ Hz lead to beam energy errors of 3 to 4 MeV at 100 GeV. The absolute normalisation of the beam energy is however always obtained from RDP calibrations and the central frequency is only used to track the evolution of the energy. Therefore systematic f^c_{RF} errors would introduce hardly any bias provided the RDP calibrations sample a LEP run evenly. Systematics deviations of f^c_{RF} would result in a scatter between RDP data and the beam energy model. If the RDP calibrations do not cover some parts of a run, the contribution of f^c_{RF} to the systematic error on the beam energy should not exceed the quoted 3 to 4 MeV.

5.1 LEP Run 1996

Operation of the LEP2 started in 1996. Detector calibrations were performed at 45 GeV with a $108^\circ/60^\circ$ optics. This optics was abandoned after a few days because its dynamic aperture was too small. LEP was then operated for most of the year with a $90^\circ/60^\circ$ optics. The beam energies were 80.5 and 86 GeV. The last two weeks of the 1996 run were used to test a $108^\circ/90^\circ$ optics. Energy calibration were performed with the $90^\circ/60^\circ$ optics. The evolution of the central frequency over the year is shown in Figure 11. The data is obtained from X_{arc} and it has been scaled to actual central frequency measurements. All data has been corrected for the evolution of horizontal corrector settings. The difference of central frequency with and without correction for the effect of correctors is shown in Figure 12. The width of the distribution is approximatively 1 Hz.

Optics	α ($\times 10^4$)	$\lvert\Delta E/\Delta f^c_{RF}\rvert$ (MeV/Hz at 100 GeV)
$60^\circ/60^\circ$	3.77	0.75
$90^\circ/60^\circ$	1.86	1.53
$101^\circ/45^\circ$	1.50	1.89
$102^\circ/90^\circ$	1.56	1.82
$108^\circ/60^\circ$	1.35	2.10
$108^\circ/90^\circ$	1.43	1.99

Table 1: Momentum compaction factor α and sensitivity of the beam energy to (central) RF frequency changes at 100 GeV. For the same phase advance α may vary by about 1% for different optics versions due to small phase adjustments.

5.2 LEP Run 1997

In 1997 LEP was operated for most of the year with a $90°/60°$ optics. During the last two weeks of the run a $102°/90°$ was tested. For most of the fills the beam energy was 91.5 GeV. Energy calibration were performed with a $60°/60°$ optics. The evolution of the central frequency over the year is shown in Figure 13. The data is obtained from X_{arc} and it has been scaled to actual central frequency measurements. All data has been corrected for the evolution of horizontal corrector settings. The difference of central frequency with and without correction for the effect of correctors is shown in Figure 14. The width of the distribution is approximatively 2 Hz.

5.3 LEP Run 1998

In 1998 LEP was operated all the year at 94.5 GeV with a $102°/90°$ optics. Energy calibration were performed with a $60°/60°$ optics. The evolution of the central frequency over the year is shown in Figure 15. The data is obtained from X_{arc} and it has been scaled to actual central frequency measurements. All data has been corrected for the evolution of horizontal corrector settings. While the central frequency measurements for electrons are in good agreement with the X_{arc} data, the measurements performed with positrons at high energy show abnormal differences with respect to the electrons and to the orbit data. No explanation for this behaviour has been found so far and the abnormal positron data has been ignored. The analysis of the resonant depolarization and NMR data seems to confirm this hypothesis. The difference of central frequency with and without correction for the effect of correctors is shown in Figure 14. The width of the distribution is approximatively 1 Hz. A small peak in the histogram corresponding to a change of approximatively -5 Hz is associated with the orbit data from the first fills in the year before day 150.

5.4 LEP Run 1999

In 1999 LEP was operated all the year with a $102°/90°$ optics. The beam energy was progressively increased from 96 to 101 GeV during the run. A new algorithm for simultaneous correction of the dispersion and the orbit (so-called Dispersion Free Steering) was used for the first time throughout the year. It resulted in smoother corrector strength distributions and in smaller corrector changes throughout the year. This lead to a significant reduction of the fill-to-fill spread of the X_{arc} measurements. Energy calibration were performed with a $60°/60°$ and a $101°/45°$ optics. The evolution of the central frequency over the year is shown in Figure 17. The data is obtained from X_{arc} and it has been scaled to actual central frequency measurements. All data has been corrected for the evolution of horizontal corrector settings. The difference of central frequency with and without correction for the effect of correctors is shown in Figure 14. The width of the distribution is approximatively 1 Hz.

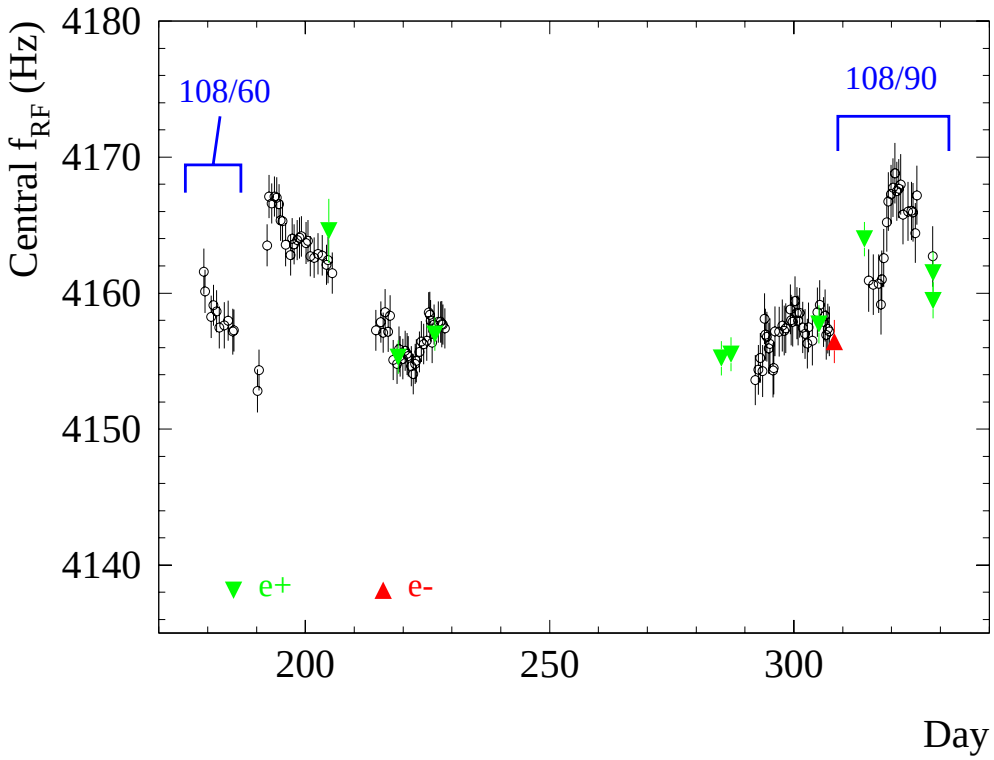

Figure 11: Evolution of the central RF frequency during the 1996 LEP run. The open points are obtained from X_{arc} and are normalised to the actual central frequency measurements (filled triangles). LEP was mostly operated with a $90°/60°$ optics, except for the first and last periods where a $108°/60°$ and a $108°/90°$ optics were tested.

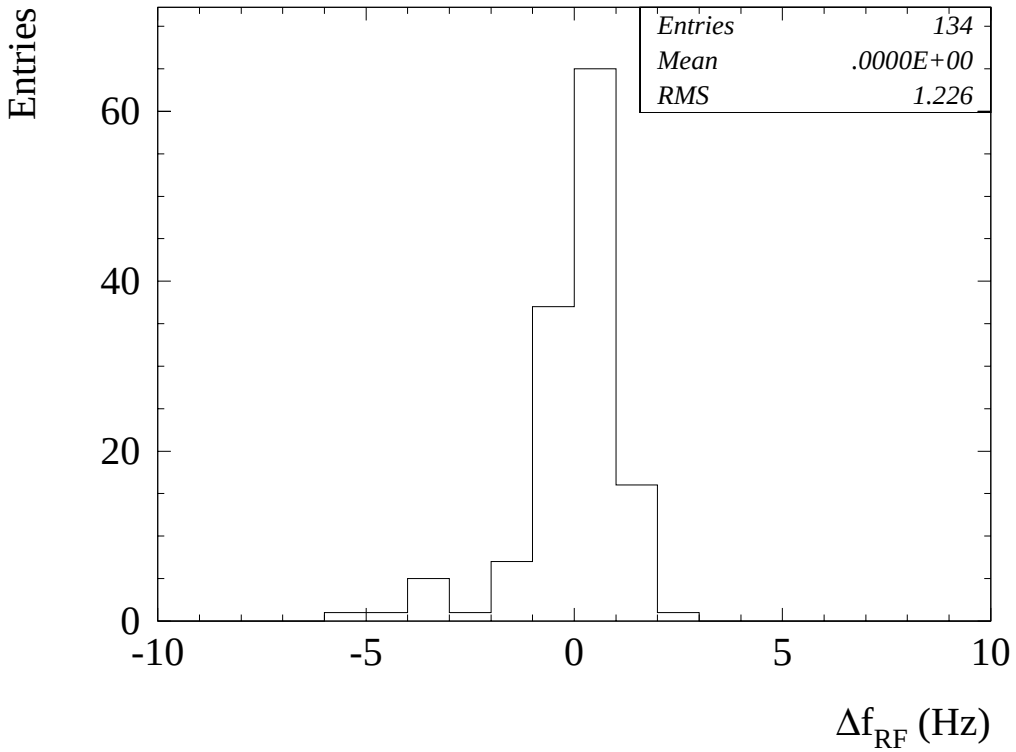

Figure 12: Distribution of the central frequency shift due to the correction for changes in corrector settings for 1996. There is one entry for each fill.

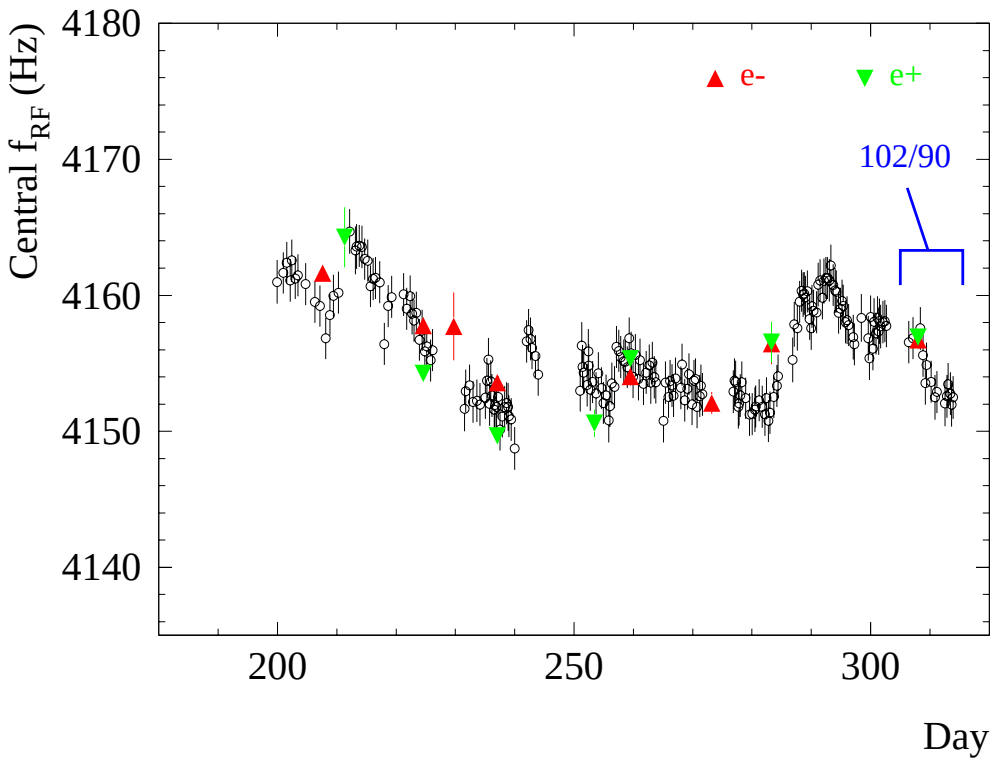

Figure 13: Evolution of the central RF frequency during the 1997 LEP run. The open points are obtained from X_{arc} and are normalised to the actual central frequency measurements (filled triangles). With the exception of the last period, LEP was operated with a $90°/60°$ optics.

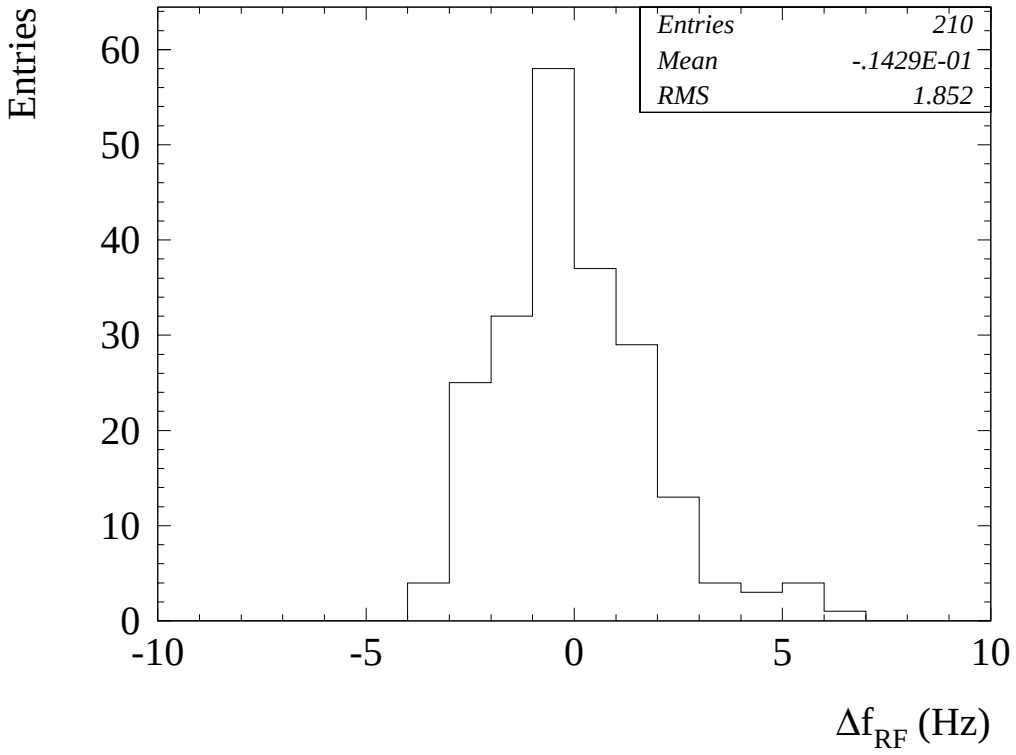

Figure 14: Distribution of the central frequency shift due to the correction for changes in corrector settings for 1997. There is one entry for each fill.

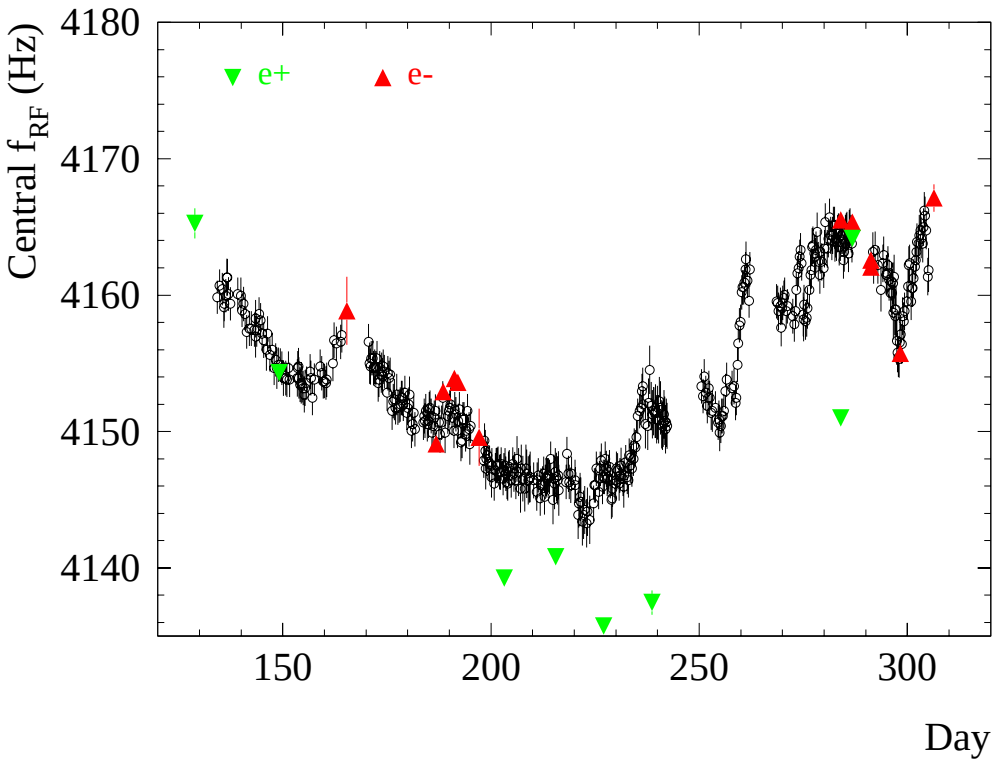

Figure 15: Evolution of the central RF frequency during the 1998 LEP run. The open points are obtained from X_{arc} and are normalised to the actual central frequency measurements (filled triangles).

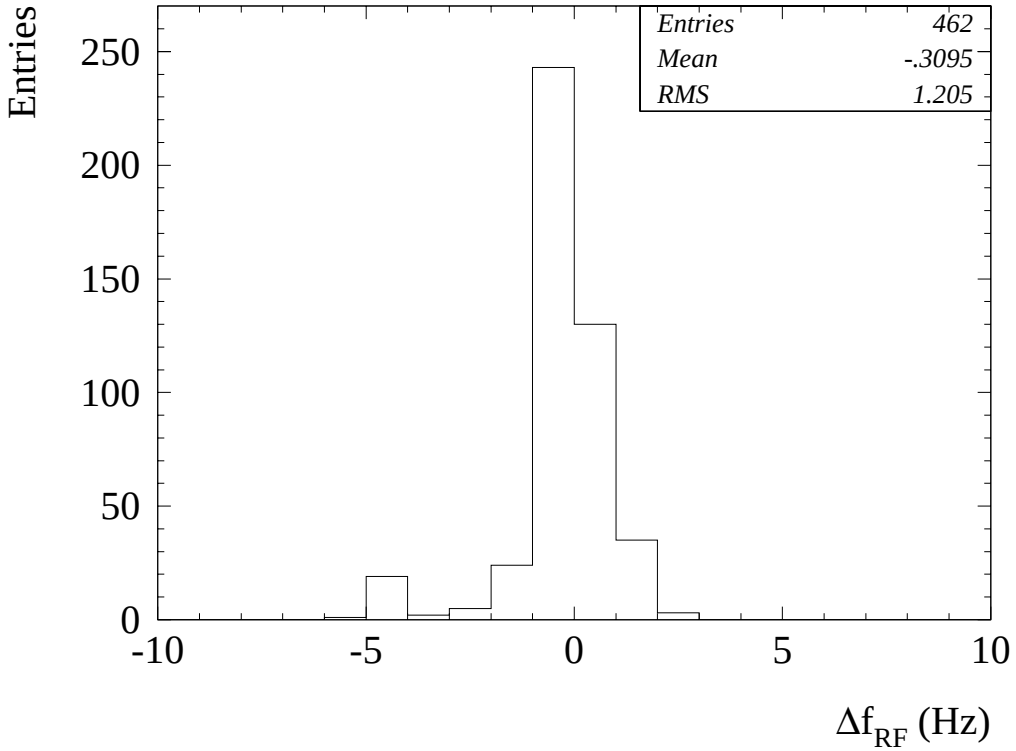

Figure 16: Distribution of the central frequency shift due to the correction for changes in corrector settings for 1998. There is one entry for each fill. The strange f^c_{RF} results for positrons have not been taken into account.

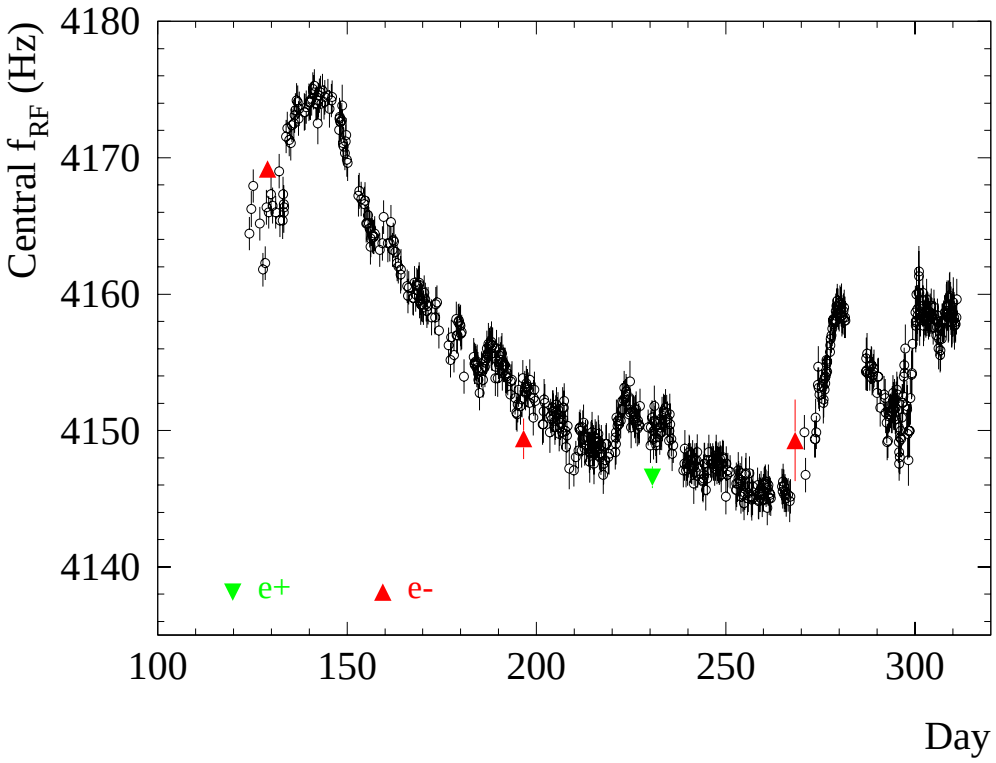

Figure 17: Evolution of the central RF frequency during the 1999 LEP run. The open points are obtained from X_{arc} and are normalised to the actual central frequency measurements (filled triangles).

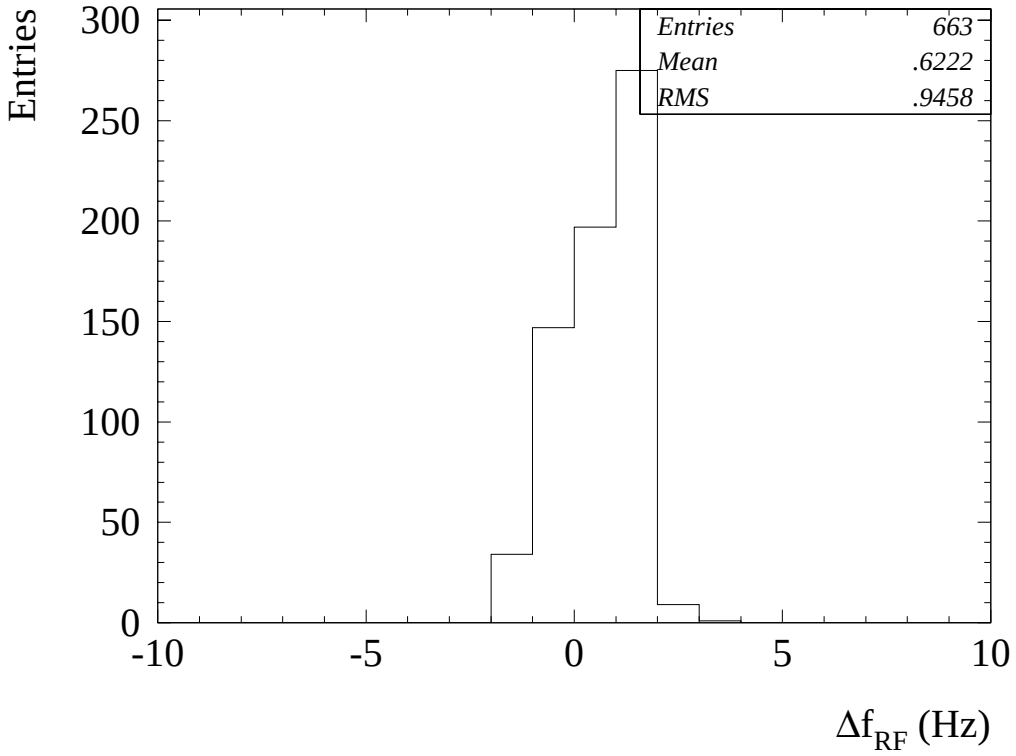

Figure 18: Distribution of the central frequency shift due to the correction for changes in corrector settings for 1999. There is one entry for each fill.

6 Summary

The influence of orbit steering on the determination of the central frequency from direct measurements and from the beam position in the LEP arcs was described by an analytical model. An important outcome of the model is the explanation of the relatively weak sensitivity of the central frequency measurement on changes of corrector settings or quadrupole movements, which is due to the good sampling of the arc orbit by the sextupoles. The validity of the model was confirmed by simulations and experiments. The central frequency data for the LEP2 runs between 1996 and 1999 was reviewed in the light of this model. The RMS spread of the corrections was in the range of 1 to 2 Hz. The corrected central frequency data exhibits a reduced fill-to-fill scatter, indicating that some of this scatter was indeed due to orbit steering. The systematic error on the central frequency over a run is estimated to be at most $\pm$ 2 Hz.

References

[1] L. Arnaudon et al., Phys. Lett. B 284 (1992) 431.
L. Arnaudon et al., Z. Phys. C 66 (1995) 45.

[2] R. Assmann et al., Z. Phys. C 66 (1995).
R. Assmann et al., Eur. Phys. J. C 6 (1999) 2, 187.

[3] A. Blondel et al., Eur. Phys. J. C 11 (1999), 573.

[4] B. Dehning, "The LEP Spectrometer", Proceedings of the IX Workshop on LEP-SPS Performance, CERN-SL-99-007 DI (1999).

[5] A. Mueller and J. Wenninger, "Energy Loss Measurements at LEP2", Proceedings of the 1999 Particle Accelerator Conference, New York, April 1999.
A. Mueller, "Energy Calibration for the Price of a Fig", Proceedings of the IX Workshop on LEP-SPS Performance, CERN-SL-99-007 DI (1999).

[6] L. Arnaudon et al., Nucl. Instr. Meth. A 357 (1995) 249.

[7] J. Wenninger, "Study of the LEP Beam Energy with Beam Orbits and Tunes", CERN SL/94-14 (BI).
J. Wenninger, "Radial Deformations of the LEP Ring", CERN SL/Note 95-21 (OP).
J. Wenninger, "Observation of radial ring deformations using closed orbits al LEP", Proceedings of the 1999 Particle Accelerator Conference, New York, April 1999.

[8] H. Schmickler, "Measurement of the Central Frequency of LEP", SL MD Note 103 (1993).

[9] A. Hofmann, "Transporting the Energy Calibration across Optics", Proceedings of the Third Workshop on LEP Performance, CERN SL/93-19 (DI).

[10] J. Wenninger, "Orbit Corrector Magnets and Beam Energy", CERN SL-Note 97-06 OP (1997).

[11] H. Grote, C. Iselin, The MAD program V8.10, CERN-SL/90-13 Rev. 3 (AP).